$^{12}C(^{12}C,^{8}Be)^{16}O$ cross-section measurement at sub-barrier energies

B. Čujec, I. Hunyadi,* and I. M. Szöghy
Laboratoire de Physique Nucléaire, Département de Physique, Université Laval, Québec, Canada G1K 7P4
(Received 11 October 1988)

Differential cross sections for the $^{12}C(^{12}C, ^{8}Be\rightarrow 2\alpha)^{16}O$ reaction have been measured at eight incident energies in the $2.43 \leq E_{c.m.} \leq 5.24$-MeV range, detecting α particles in 200-μm thick Makrofol polycarbonate foils, which were subsequently carefully etched and scanned under microscope for the $^{8}Be\rightarrow 2\alpha$ group and the α groups from the $^{12}C(^{12}C, \alpha)^{20}Ne$ reaction. The ^{8}Be channel cross section, ranging between 4×10^{-4} μb and 280 μb, is smaller for $E_{c.m.} \geq 3.91$ MeV, but larger for $E_{c.m.} \leq 3.13$ MeV than the $\alpha_0+^{20}Ne_{g.s.}$ channel cross section. The $^{12}C(^{12}C, ^{8}Be)^{16}O$ cross section is well reproduced by the distorted-wave Born approximation calculation of a direct α-transfer reaction down to $E_{c.m.}=3.91$ MeV. In the $3.13 \geq E_{c.m.} \geq 2.43$-MeV range, however, the measurements exceed the distorted-wave Born approximation prediction by one to three orders of magnitude. It is suggested that the formation of ^{12}C-^{12}C dinuclear states, favoring an α transfer, becomes a predominant process at incident energies $E_{c.m.} \leq 3.13$ MeV.

I. INTRODUCTION

The $^{12}C+^{12}C$ system has been extensively studied at the energies around and below the Coulomb barrier mainly for two reasons: (1) the existence of uniquely prominent intermediate structure resonances observed[1] as early as in 1960, but which are still not completely understood, and (2) the importance of this reaction for the stellar evolution and nucleosynthesis in the carbon burning phase. To obtain the astrophysically important information, the cross sections for the $\alpha+^{20}Ne$ and $p+^{23}Ne$ channels have been measured down to $E_{c.m.} \approx 3$ MeV, detecting either the charged particles (α's and protons)[2,3] or γ rays emitted from residual nuclei.[4,5]

The $^{12}C(^{12}C, ^{8}Be)^{16}O$, $^{8}Be\rightarrow 2\alpha$ reaction has been measured only at higher energies, in view of studying the resonance structure: For $E_{c.m.}=9-20$ MeV by Fletcher *et al.*[6] with coincident detection of the two α particles, for $E_{c.m.}=6-11$ MeV by Wada *et al.*[7] with detection of ^{16}O nuclei, and recently for $E_{c.m.}=5-7$ MeV by Sprengel *et al.*[8] with coincident detection of the two α particles in a large annular detector split into two isolated halves. A prominent resonance structure has been observed and several new resonances established in these studies. By lowering the energy, the measurement of this reaction becomes increasingly more difficult due to the low energy of the α particles from ^{8}Be disintegration (the reaction's Q value is -0.205 MeV), the smallness of cross section, and the huge number of elastically scattered ^{12}C nuclei. For the astrophysically interesting region, $E_{c.m.}=1-5$ MeV, Kozlowski[9] estimated the $^{12}C(^{12}C, ^{8}Be)^{16}O$ cross section with a subbarrier α-transfer calculation, finding it to be small with respect to the measured and extrapolated total reaction cross section. However, as the cross section for the α transfer between two ^{12}C nuclei could be enhanced by the formation of a ^{12}C-^{12}C dinuclear state,[10] and as a substantial enhancement has in fact been observed[11] at subbarrier energies in α-transfer reactions from ^{9}Be, the measurement of the $^{12}C(^{12}C, ^{8}Be)^{16}O$ cross section at subbarrier energies is highly desirable.

In the present work we have measured the $^{12}C(^{12}C, ^{8}Be)^{16}O$ cross section between $E_{c.m.}=2.43$ and 5.24 MeV, detecting the α particles in a plastic foil sensitive to α particles and heavier ions only. The advantage of a plastic track detector over a silicon one is its insensitivity to the electrons and the electric fields produced by the scattered ^{12}C ions stopped in an absorber placed before the detector. A plastic foil can also be bent into a cylindrical shape, thus allowing a simultaneous detection of the emitted particles in the whole angular range. An absorber with thickness carefully adjusted so that at each angle it stopped the elastically scattered ^{12}C, but transmitted the alphas from ^{8}Be disintegration, was placed before the detector. The individual α-particle groups from the $\alpha+^{20}Ne$ and $^{8}Be+^{16}O$, $^{8}Be\rightarrow 2\alpha$ channels were easily resolved in the process of the subsequent etching and scanning. The fact that the two α particles from ^{8}Be disintegration were not detected in coincidence did not present a serious problem since the yield from other channels in the energy range of the $^{8}Be\rightarrow 2\alpha$ group was not large and could be subtracted away. The yield of α particles from the sequential decay ^{20}Ne (5.62, 5.79 MeV)$\rightarrow\alpha''_{4,5}+^{16}O$ (see Fig. 1), which is included in the $^{8}Be\rightarrow 2\alpha$ group, could be evaluated from the measured $\alpha_{4,5}+^{20}Ne$ (5.62, 5.79 MeV) channel cross section for incident energies up to $E_{c.m.}=5.24$ MeV. At higher incident energies, ^{20}Ne states with excitation energy $E_x \geq 6.72$ MeV become populated, blurring the distinction between the $^{8}Be\rightarrow 2\alpha$ and other groups. Therefore, our measurement of the $^{12}C(^{12}C, ^{8}Be)^{16}O$ cross section was limited to the incident energies $E_{c.m.} \leq 5.24$ MeV. Some preliminary results of the present work were already reported.[12]

II. EXPERIMENTAL METHOD

The measurements were performed using the $^{12}C^{+}$ and $^{12}C^{++}$ beams of the 7.5 MeV Van de Graaff accelerator

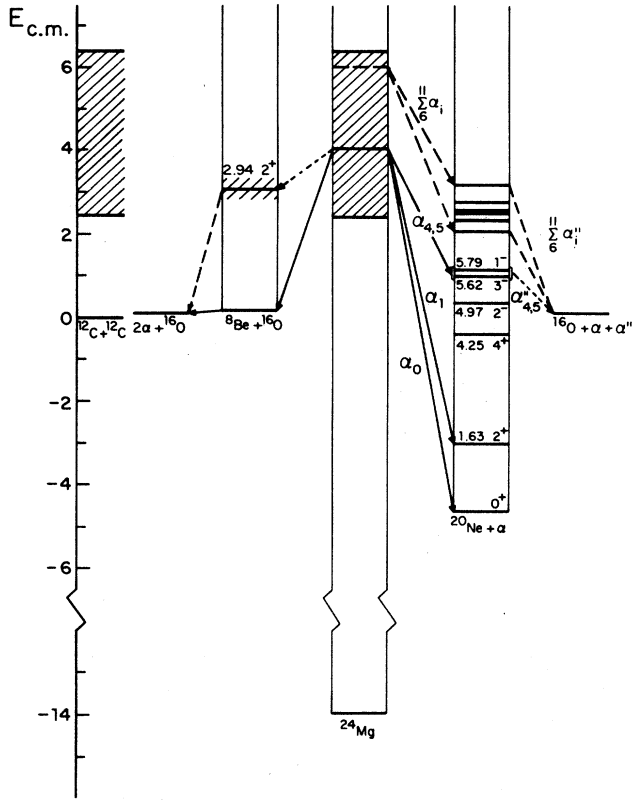

FIG. 1. Energy-level diagram for the α-particle channels of the $^{12}C+^{12}C$ reaction. The energy region and the α groups investigated in the present work are indicated by crosshatching and solid arrows, respectively.

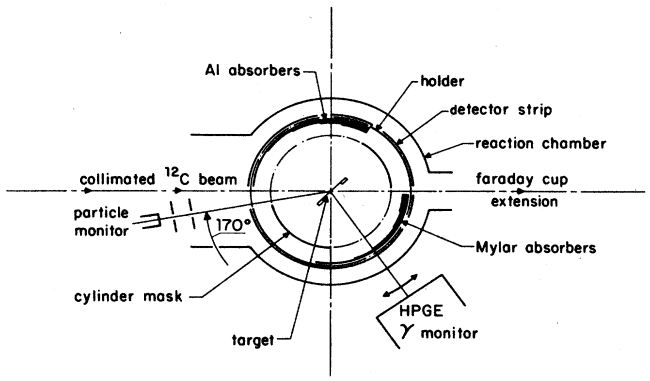

FIG 2. Schematic view of the reaction chamber used for the exposure of the Makrofol detectors.

of Université Laval. The targets were 30 $\mu g/cm^2$ thick ultrapure (99.9995%) natural carbon foils, purchased from Atomic Energy of Canada Ltd. They were transferred from the glass to the aluminum target frame by floatation on distilled and deionized water. The α particles, produced in the $^{12}C+^{12}C$ reaction, were detected in a 200-μm thick and 13-mm wide polycarbonate foil (Makrofol-E) sensitive to alphas and heavier ions. This plastic detector strip was bent into a cylinder of 4-cm radius, with transmission holes 6 mm in diameter, punched at 0°, 170°, and 180° with respect to the direction of the beam. The $^{8}Be\rightarrow 2\alpha$ and $\alpha_{4,5}$ groups (see Fig. 1) were detected in the forward part of the strip and the α_0 and α_1 groups in its backward part.

The reaction chamber is shown in Fig. 2. In the target holder were mounted three targets which were exchanged and oriented from the bottom. Three rings, each holding a Makrofol-detector strip, could be exchanged and oriented from the top of the chamber. The outside of each ring was grooved all around to hold together the Makrofol strip and a protective foil. The aluminum and Mylar (Somar, NY) absorbers were glued by epoxy on the graduated interior of each ring. In order to reduce the background counts from the scattered beam and to protect the unexposed detector strips, a cylindrical mask with grooved slits subtending a slightly greater solid angle than that of the holder was positioned between the target and the detector. Some scattered particles could still enter the detector but only at an oblique angle, thus producing a distinguishable, noncircular track shape. The transmission of the analyzed beam through the collimator and the reaction chamber was achieved with less than a 5% loss. The focusing of the beam was verified, at each bombarding energy, with transparent tapes positioned at the entrance and the exit of the reaction chamber and at the target position.

The incident beam was monitored at the target and at the Faraday cup in order to observe the ratio of the two currents, which provided an easy check for target deterioration. Moreover, the particle and the γ-ray yields were detected with a small silicon detector at 170° and with a 80-cm^3 high purity germanium (HPGe) detector at 55°, respectively. These two detectors permitted the observation of characteristic particle groups and γ rays (from the $\alpha+^{20}Ne$ and $p+^{23}Na$ channels) at all bombarding energies, except at the lowest one at 5 MeV ($E_{c.m.}=2.43$ MeV in the center of the target), where the characteristic α particles and γ rays were completely masked by the detector noise and the background radioactivity.

The absorbers placed before the Makrofol detector were chosen to stop the elastically scattered ^{12}C particles but to transmit the $^{8}Be\rightarrow 2\alpha$ group in the forward part of the strip, and to stop the α_2 group in the backward part of the strip. A set of Mylar and aluminum absorbers of thicknesses carefully chosen and varying with angle was prepared for each bombarding energy, considering the kinematic and stopping power conditions, as illustrated in Fig. 3.

The measurements were performed with a $^{12}C^{+}$ beam at 5-, 6-, and 6.41-MeV bombarding energies ($E_{c.m}=2.425$, 2.93, and 3.13 MeV) and with $^{12}C^{++}$ beam at seven bombarding energies between 7.95 and 12.86 MeV ($3.91\leq E_{c.m.}\leq 6.37$ MeV). The atomic beam intensities at the target were typically 1 μA for $^{12}C^{+}$ and 100 nA for $^{12}C^{++}$. The exposure time was selected so as to obtain a track density of 50 to 400 tracks/mm^2 and was estimated beforehand from short test runs, principally

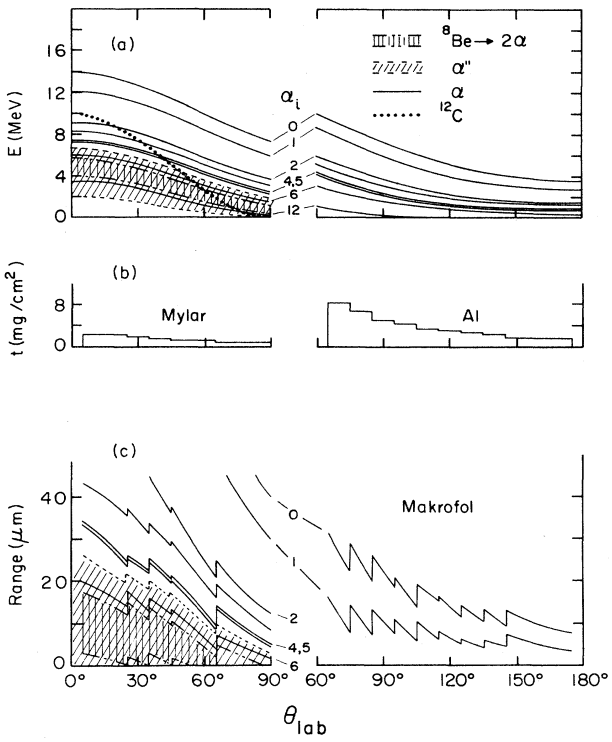

FIG. 3. Kinematical conditions and the effect of absorbers for the exposure at 10 MeV beam energy ($E_{c.m.}$ =4.99 MeV). (a) The angular dependence of the kinetic energy for the various α-particle groups and for the elastically scattered ^{12}C. (b) The thickness of the absorber placed before the Makrofol detector at various angles. (c) The expected range in the Makrofol for the various α-particle groups.

taken to check the absorbers. The exposure time had to be increased by orders of magnitude at decreasing bombarding energies due to the rapid decrease of cross section, e.g., a 1-h run at 10-MeV bombarding energy was equivalent to a 2-day run at 5-MeV bombarding energy. In the latter case, the targets deteriorated in a predictable way and had to be replaced after 5 h of irradiation.

The etching of Makrofol-E strips was performed at controlled temperature (70.0±0.1 °C) in the etchant solution (30 g KOH+90 ml H_2O+100 ml C_2H_5OH), as recommended by Somogyi *et al.*,[13] with a surface removal rate of about 20 μm/h. The action of the solution was periodically checked by etching detector samples irradiated with alpha particles from an ^{241}Am source. The scanning of Makrofol strips was made under a microscope in 0.42- or 0.26-mm wide bands, depending on track density, counting the tracks of a given diameter. The different α-particle groups were recognized by the characteristic variation of the track diameter with subsequent etching.[13] The tracks of a given α group appear first with a small diameter. The diameter increases with more etching, the removal of the plastic material at the track being faster than at the rest of the surface. The tracks fade away when the layer corresponding to the α-particle range is removed. Typically, two α groups with an energy difference of ~0.3 MeV were easily distinguished. The conversion of the linear dimension of the strip into the corresponding angle with respect to the beam direction was achieved by means of the circular beam marks at 0° and 180°.

III. RESULTS AND DISCUSSION

The angular distributions of the α particles from the ^{12}C(^{12}C, ^{8}Be→2α)^{16}O and ^{12}C(^{12}C,α)^{20}Ne reactions were obtained as described in the previous section, at eight bombarding energies, ranging from 5.00 to 10.50 MeV ($2.43 \leq E_{c.m.} \leq 5.24$ MeV). Figure 4 shows the results of the track scanning for three representative bombarding energies. As all reaction channels were measured during the same exposure, the track density is indicative as well of the angular distribution (in the laboratory system) as of the relative cross section for a given bombarding energy. As Fig. 4 shows, the group A, containing alphas from the ^{8}Be→2α disintegration, is strongly peaked forward and its cross section increases relative to that of α_0 and α_1, while that of $\alpha_{4,5}$ decreases with decreasing bombarding energy.

The center-of-mass differential cross sections for two-body reaction channels are expressed by the Legendre polynomial expansion, $d\sigma/d\Omega = \sum_k a_k P_k(\cos\theta)$, with only even k because of identical particles in the incident channel, and the integrated cross section is then given by $4\pi a_0$.

For the α+^{20}Ne channels, the coefficients a_k were obtained simply by the least-square fitting of the experimental data transformed to the center-of-mass system. For the (^{8}Be→2α)+^{16}O channel, the center-of-mass differential cross sections were obtained in two ways. (1) As the disintegration energy for ^{8}Be→2α is small (92 keV) with respect to the kinetic energy of ^{8}Be, it was assumed that the ^{8}Be angular distribution (in the laboratory system) is given simply by the measured α-particle distribution (group A in Fig. 4) divided by two. The transformation from the laboratory to the center-of-mass system was thus reduced to a simple two-body analysis. (2) A Monte Carlo simulation method was developed[14] which took into account the isotropic disintegration of the recoiling ^{8}Be as well as the effects of the target and absorber thicknesses, and the threshold for α-particle counting (E_α=0.1 MeV) in the Makrofol foil. Moreover, the contribution of the α-particles from the sequential emission ^{20}Ne (5.62, 5.79 MeV)→$\alpha''_{4,5}$+^{16}O, which occurs with 50% probability (50% is γ disintegration) and is included in group A, was also evaluated by the Monte Carlo simulation from the measured $\alpha_{4,5}$+^{20}Ne (5.62, 5.79 MeV) differential cross section and subtracted away. As the collected charge did not provide a reliable measure at low energies, where the targets broke several times, we normalized our cross-section data to the α_0 cross sections reported by Becker *et al.*[3]

The results of this analysis are presented in Figs. 5–11 and in Tables I and II. In Fig. 5 we compare the differential cross sections for the α_0 channel with those measured previously in our laboratory[15] with silicon detectors in a large (50-cm diameter) scattering chamber.

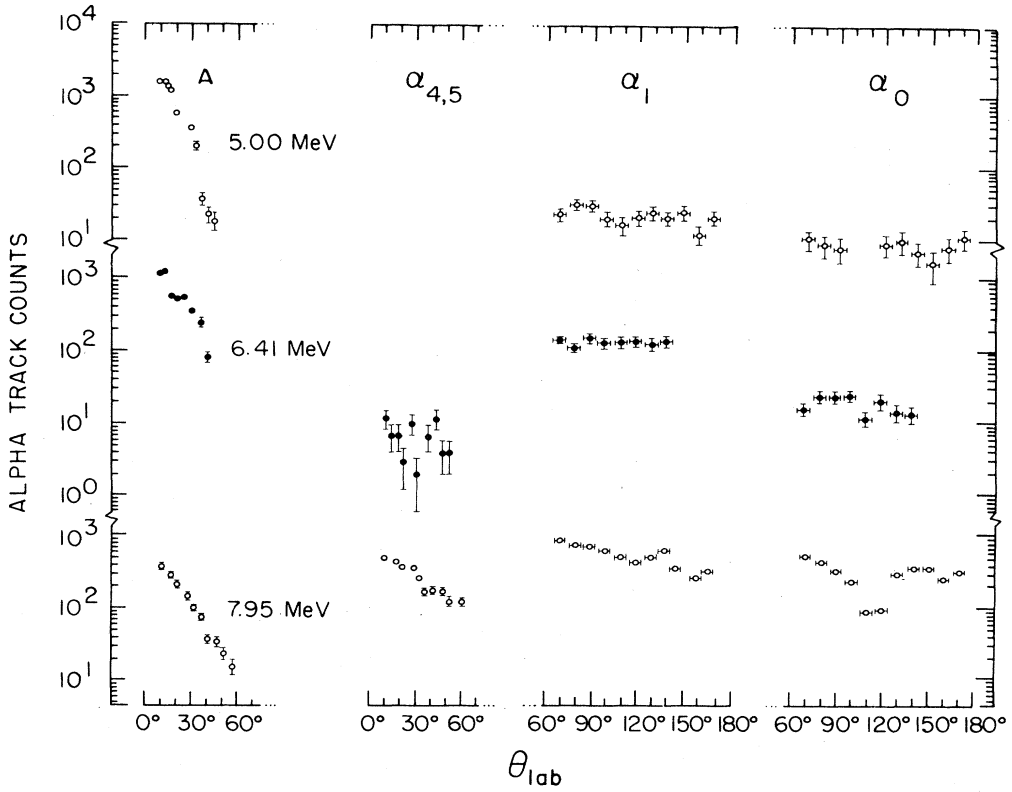

FIG. 4. Angular distributions (laboratory system) for the various α-particle groups, measured at beam energies of 5 MeV ($E_{c.m.}=2.435$ MeV), 6.41 MeV ($E_{c.m.}=3.13$ MeV), and 7.95 MeV ($E_{c.m.}=3.91$ MeV). The group A contains α particles from the $^{8}Be_{g.s.}$ disintegration. The statistical errors are shown when exceeding the size of the circle.

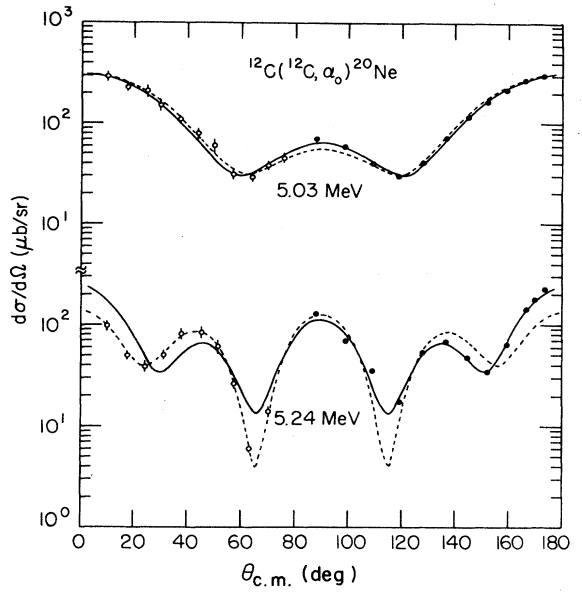

FIG. 5. Angular distributions (c.m.) for the $^{12}C(^{12}C,\alpha_0)^{20}Ne$ reaction measured in the present work at $E_{c.m.}=5.03$ MeV and $E_{c.m.}=5.24$ MeV with a 30-μg/cm^2 target (full circles and full curve) in comparison with those measured by Dasmahapatra *et al.*[15] at $E_{c.m.}=5.02$ and $E_{c.m.}=5.25$ MeV with a 10-μg/cm^2 target (empty circles and dashed curve).

Considering the differences in the c.m. incident energies (5.03 MeV vs 5.02 MeV and 5.24 MeV vs 5.25 MeV) and in the target thicknesses (30 μg/cm^2 vs 10 μg/cm^2) used presently and previously, the agreement between the two measurements is satisfactory. To situate the present measurements with respect to the known resonance structure,

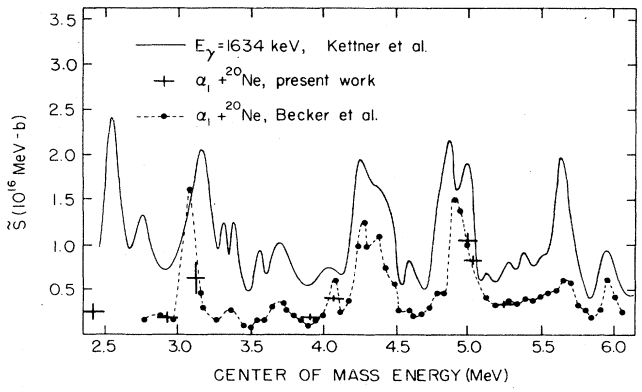

FIG. 6. $\tilde{S}$ factor, $\tilde{S}=\sigma E\exp(87.21/E^{1/2}+0.46E)$, for the α_1+^{20}Ne as measured in the present work (crosses, indicating errors) and by Becher *et al.*[3] The $\tilde{S}$ factor for the ^{20}Ne 1.634-MeV γ-ray measured by Kettner *et al.*[5] is also shown.

TABLE I. Angular distributions in the c.m. for the $^8Be+^{16}O$ and $\alpha+^{20}Ne$ channels. Coefficients a_k in expansion $\sum_k a_k P_k(\cos)$ with $a_0=1$.

	$^8Be+^{16}O$[a]		$\alpha_0+^{20}Ne_{g.s.}$				$\alpha_1+^{20}Ne$ (1.63 MeV)				$\alpha_{4,5}+^{20}Ne$ (5.62, 5.79 MeV)	
$E_{c.m.}$ (MeV)	a_2	a_4	a_2	a_4	a_6	a_8	a_2	a_4	a_6	a_8	a_2	a_4
2.425	2.86	1.62	0.22	−0.05			0.32	−0.01				
2.93	1.25	−1.01	0.27	−0.65			0.09	0.49			0.08	0.54
3.13	1.71	0.36										
3.91	1.62	0.27	0.42	1.13	−0.44	−0.78					0.83	
4.07	1.59	−0.37	−0.78	1.20			0.04	−0.23	0.34		0.50	
4.99	0.77	1.28	1.63	1.47			0.90	1.16			1.07	0.29
5.03	0.81	1.69	1.49	1.47			0.47	1.22			0.85	0.28
5.24	−0.25	0.78	0.18	1.29	−0.23	1.88	−0.87	0.81	−0.23	0.35	0.36	0.36

[a] Monte Carlo simulation coupled with $\alpha''_{4,5}$ subtraction.

Fig. 6 shows, in the form of astrophysical $\tilde{S}$ factor

$$\tilde{S}=\sigma E \exp(87.21/E^{1/2}+0.46E) ,$$

the cross sections obtained for the α_1 channel along with those of Becker *et al.*[3] and the cross sections for the ^{20}Ne 1.63 MeV γ ray measured by Kettner *et al.*[6] The agreement between the two α_1 cross-section measurements is excellent.

The Monte Carlo simulation results for the $^{12}C(^{12}C, ^8Be\rightarrow 2\alpha)^{16}O$ reaction are illustrated in Fig. 7, showing the detection efficiency for the $^8Be\rightarrow 2\alpha$ group at incident energy $E_{c.m.}=2.43$ MeV. The plummeting of efficiency beyond $\theta_{lab}=60°$ explains why no tracks were observed for $\theta_{lab}\geq 60°$. Figures 8 and 9 show the differential cross sections for the $^{12}C(^{12}C, ^8Be)^{16}O$ reaction in the laboratory and the c.m. systems, respectively. In Fig. 8, the full circles show the experimental data and the crosses show the laboratory differential cross sections after the yield $\alpha''_{4,5}$, evaluated by the Monte Carlo simulation, has been subtracted away. At the three lowest incident energies, the cross sections for the $\alpha_{4,5}+^{20}Ne$ (5.62, 5.79 MeV) channel are too small to produce any visible contribution of $\alpha''_{4,5}$, while at higher incident energies the $\alpha''_{4,5}$ contribution accounts for about half of the counts of group A. The solid curves show the Monte Carlo simulation results. In Fig. 9, the full circles show the results of the simple two-body analysis. The difference between the c.m. cross sections obtained by the two-body analysis (dashed curves) and by the Monte Carlo simulation (solid curves) is due mainly to the fact that in the former case the $\alpha''_{4,5}$ contribution is included, while in the latter it is subtracted away. The c.m. differential cross sections are, of course, symmetrical around 90° because of identical particles in the incident channel and are, in general, strongly peaked forward. The Legendre polynomial expressions include terms up to $k=4$ only (Table I), indicating that only the $l=0$ and $l=2$ incident partial waves are involved, and this even at $E_{c.m.}=5.24$ MeV, where the $\alpha_0+^{20}Ne$ channel indicates the presence of a $J=4^+$ resonance.[15]

The $^{12}C(^{12}C, ^8Be)^{16}O$ integrated cross sections, as obtained with the Monte Carlo simulation analysis, are presented in Table II. Figure 10 compares these ^8Be cross sections with the α_0 cross sections of Becker *et al.*[3] and with the total reaction cross section measured[4] by the total γ-ray yield method. As we see, the measured ^8Be cross section has an unusual energy dependence. The two measurements at $E_{c.m.}\approx 4$ MeV indicate a very steep decrease, while the measurements at $E_{c.m.}\approx 3$ and 2.43 MeV indicate that the ^8Be cross section is decreasing more slowly than the α_0 cross section. Though a change in the slope is possible if a different reaction mechanism sets in, we rather first examine carefully the possibility of spurious counts in either the $^8Be\rightarrow 2\alpha$ or the α_0 group, which served for normalization.

First we note that the $^{12}C^+$ beam was used for the mea-

TABLE II. Cross sections for the $^8Be+^{16}O$ and $\alpha+^{20}Ne$ channels.

$E_{c.m.}$	Relative cross section[a]				Cross sections in μb			
(MeV)	^8Be	α_0	α_1	$\alpha_{4,5}$	^8Be	α_0^b	α_1	$\alpha_{4,5}$
2.425	6.6	1	2.7		4.0×10^{-4}	0.6×10^{-4}	1.6×10^{-4}	
2.93	5.4	1	1.8	0.10	3.8×10^{-2}	0.7×10^{-2}	1.3×0^{-2}	0.07×10^{-2}
3.13	3.1	1	8.1	0.10	7.5×10^{-2}	2.4×10^{-2}	2.0×10^{-2}	0.25×10^{-2}
3.91	0.033	1	2.0	0.32	0.10	3.0	6.1	0.97
4.07	0.046	1	1.4	0.53	0.83	18	26	9.4
4.99	0.32	1	3.0	1.5	260	800	2400	1220
5.03	0.34	1	3.1	1.4	240	700	2100	980
5.24	0.50	1	3.0	1.8	280	560	1700	980

[a] With respect to the cross section for the $\alpha_0+^{20}Ne$ channel.
[b] The cross sections of Becker *et al.*,[3] serving for normalization.

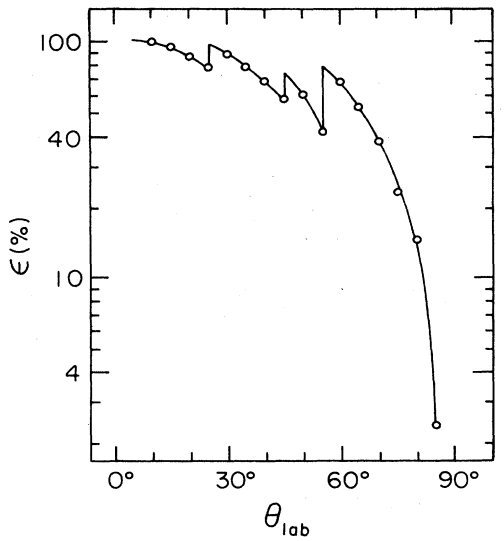

FIG. 7. Detection efficiency for the α particles from the ^{8}Be breakup, evaluated by the Monte Carlo simulation, for the exposure at $E_{c.m.}=2.43$ MeV. The discontinuities at $\theta_{lab}=25°$, 45°, and 55° are due to the discontinuities in the absorber thickness.

surements at $E_{c.m.} \leq 3.13$ MeV and the $^{12}C^{++}$ beam for the measurements at $E_{c.m.} \geq 3.91$ MeV. As $^{6}Li^{+}$ has the same Z/M ratio as $^{12}C^{++}$ ($Z/M=\frac{1}{6}$), there exists a possibility of a $^{6}Li^{+}$ admixture into the $^{12}C^{++}$ beam, while the $^{12}C^{+}$ beam should be pure, since there are no other light ions with the $Z/M=\frac{1}{12}$ ratio. For the measurements at $E_{c.m.} \approx 4$ MeV, the α particles from the reactions $^{12}C(^{6}Li,\alpha)^{14}N$ (3.95 MeV) ($Q=4.85$ MeV) at $E_{lab}(^{6}Li)=4$ MeV and $^{12}C(^{12}C,\alpha_0)^{20}Ne_{g.s.}$ ($Q=4.62$ MeV) at $E_{lab}(^{12}C)=8$ MeV have practically the same energy at the backward angles, where the α_0 group was measured. As the cross section for the $^{12}C(^{6}Li,\alpha)^{14}N(3.95$ MeV) reaction at $E_{lab}(^{6}Li)=4$ MeV is 3.5 mb (Ref. 16), while that for the $^{12}C(^{12}C,\alpha_0)^{20}Ne_{g.s.}$ reaction at $E_{lab}(^{12}C)=8$ MeV is only 8 μb, the cross-section ratio is $(^{6}Li+^{12}C \rightarrow \alpha+^{14}N)/(^{12}C+^{12}C \rightarrow \alpha_0+^{20}Ne)=440$. A $\sim 1\%$ admixture of $^{6}Li^{+}$ into the $^{12}C^{++}$ beam would produce a large number of spurious counts in the α_0 group and thus, because of our normalization of the ^{8}Be-channel cross section to the α_0-channel cross section, would result in a too low ^{8}Be-channel cross section at $E_{c.m.} \approx 4$ MeV. To verify this possibility, we normalized the ^{8}Be cross sections with the ^{20}Ne 1.63 MeV γ-ray yields, measured in the HPGe detector, using the ^{20}Ne 1.63-MeV γ-ray cross sections of Kettner *et al.*,[5] shown in Fig. 6. So normalized, the cross sections agree with those normalized with the α_0 cross sections. Moreover, as the γ ray from the ^{14}N 2.31-MeV$\rightarrow$0 transition does not appear in the HPGe spectra, we consider the effect of the $^{6}Li^{+}$ admixture in the $^{12}C^{++}$ beam as improbable.

For the measurements at $E_{c.m.} \leq 3.13$ MeV, all tracks in the A group were assigned to the $^{8}Be \rightarrow 2\alpha$ disintegration, while at $E_{c.m.} \geq 3.91$ MeV the contribution from the $^{20}Ne(5.62,\ 5.72\ \text{MeV}) \rightarrow \alpha''_{4,5}+^{16}O$ sequential decay was subtracted away. As Table II shows, with decreasing energy, the $\alpha_{4,5}$ cross section decreases rapidly with respect to the α_0 cross section and becomes negligible at

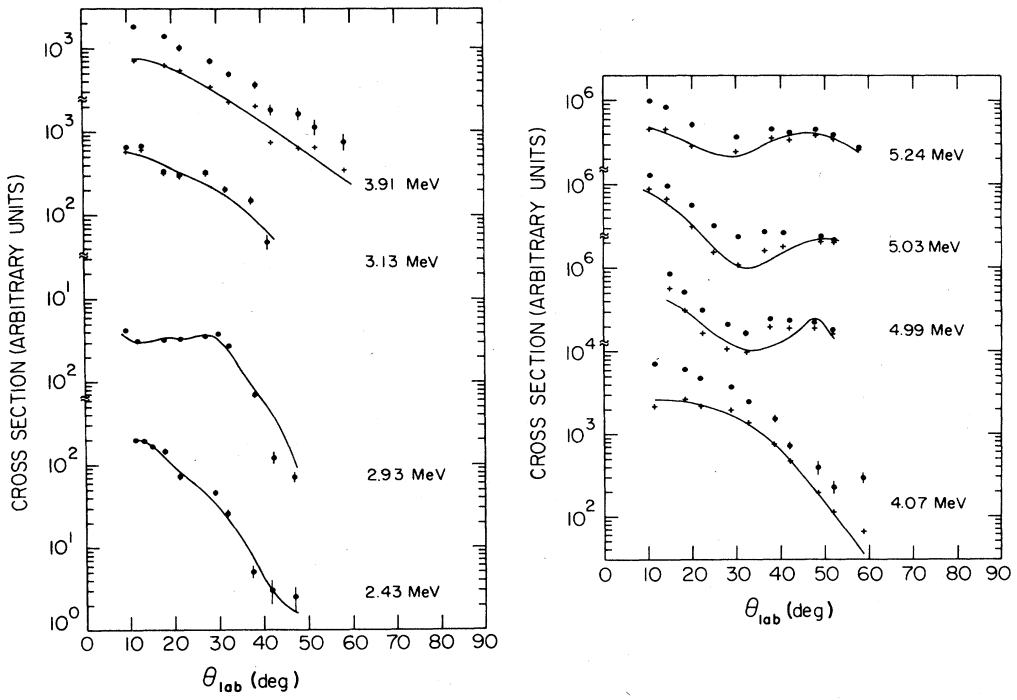

FIG. 8. Measured differential cross sections (laboratory system) for $^{8}Be \rightarrow 2\alpha$ group before (full circles) and after the $\alpha''_{4,5}$ yield subtraction (crosses). The curves show the Monte Carlo simulation results. The incident c.m. energies are given.

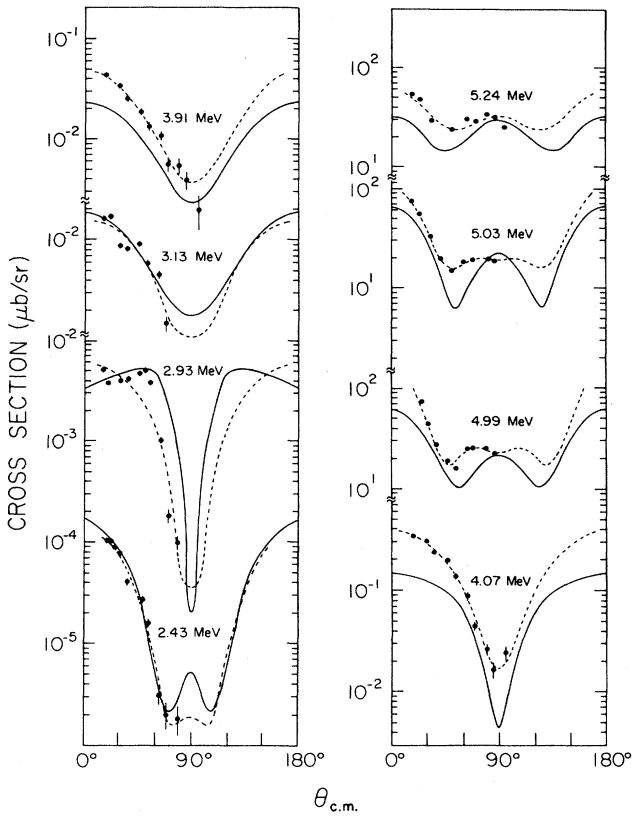

FIG. 9. Center-of-mass cross sections for the ^{8}Be channel. The solid curves are the Monte Carlo simulations, obtained after the $\alpha''_{4,5}$-yield subtraction, and correspond to the curves in Fig. 8. The points were obtained from the laboratory yields by a simple two body analysis. The dashed curve is a Legendre polynomial fit to the points. The incident c.m. energies are given.

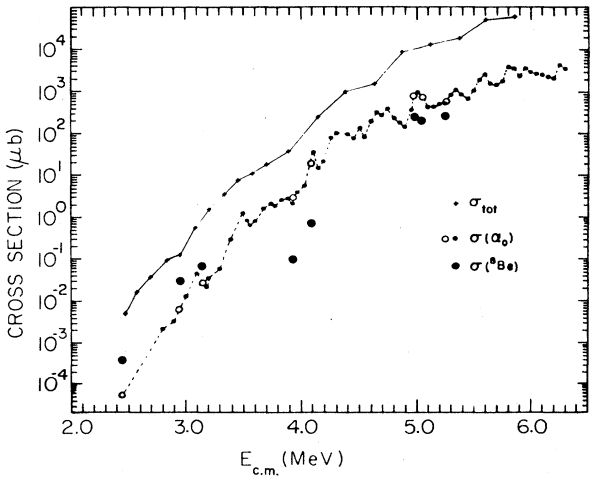

FIG. 10. ^{12}C(^{12}C,^{8}Be)^{16}O cross section measured in the present work (large full circles) in comparison with the ^{12}C(^{12}C,α_0)^{20}Ne cross section of Becker *et al.*[3] (small full circles) and the ^{12}C+^{12}C total reaction cross sections of High and Čujec[4] (crosses). The large empty circles show the interpolated and extrapolated values used in the normalization. The lines serve to guide the eye.

$E_{\text{c.m.}} \leq 3.13$ MeV. This is understandable since the c.m. energy in the outgoing channel, $\alpha_{4,5}+^{20}$Ne, decreases below $\frac{1}{3}$ of the ($\alpha+^{20}$Ne) Coulomb barrier. For the measurements at $E_{\text{c.m.}} M = 3.13$ MeV, the assumption that the $\alpha''_{4,5}$ contribution to the A group is negligible thus seems to be justified. It is possible that for the measurements at $E_{\text{c.m.}} \approx 4$ MeV, the $\alpha_{4,5}$ contribution, which amounted to about half of the total counts in the A group, was overestimated. However, even if we treat the measurements at $E_{\text{c.m.}} \approx 3$ MeV and $E_{\text{c.m.}} \approx 4$ MeV in the same way regarding the $\alpha''_{4,5}$ subtraction, the ^{8}Be cross section at either energy shift only by a factor of ~ 2, and the marked effect in the energy dependence, though diminished, is still there. This is illustrated in Fig. 11, where the different evaluations of the integrated ^{8}Be cross section are presented: Those evaluated by the two-body analysis (without $\alpha''_{4,5}$ subtraction) and those evaluated by the Monte Carlo simulation method (with $\alpha''_{4,5}$ subtraction), normalized either to α_0 cross sections or to ^{20}Ne 1.63-MeV γ-ray cross sections.

Finally we examine the possibility of spurious tracks in the $^8\text{Be} \rightarrow 2\alpha$ group, arising from contaminants in the target. The carbon foils used for the targets were of high purity (99.9995%); the analysis of the producer (Atomic Energy of Canada) showed only traces of elements heavier than Mg, and we manipulated the foils very care-

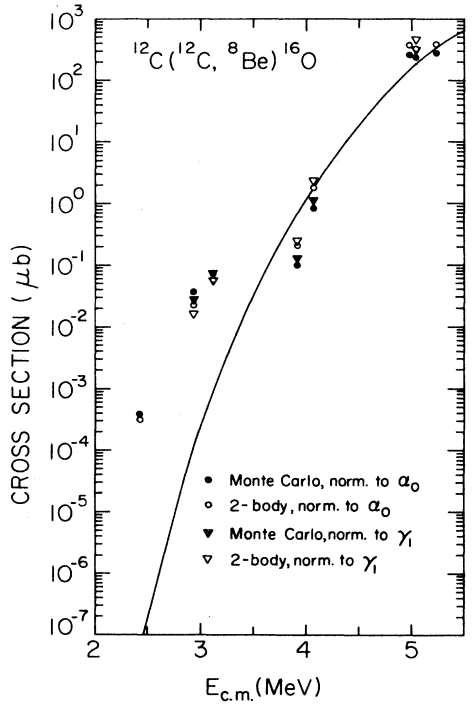

FIG. 11. ^{12}C(^{12}C,^{8}Be)^{16}O cross sections as obtained with the simple two-body analysis (empty circles and triangles) and with the Monte Carlo simulation method including $\alpha''_{4,5}$ subtraction (full circles and triangles), normalized either with α_0-channel cross sections (circles) or with the ^{20}Ne 1.63-MeV γ-ray yields (triangles). The curve shows the DWBA calculation for a direct α-transfer reaction.

fully. Nevertheless, even a very small amount of elements with $Z<6$ could contribute a relatively large number of spurious counts at the lowest measured energies since for these nuclei the cross section is not suppressed as much by the Coulomb barrier as it is for ^{12}C. To investigate this possibility we bombarded ^{11}B, ^{9}Be, and Li targets with a $^{12}C^{+}$ beam using the same conditions (beam energy, absorbers, detectors, etc.) as for the $^{12}C+^{12}C$ measurement at $E_{lab}=5$ MeV. The Makrofol detectors were examined in particular for the α tracks in the energy range of the $^{12}C(^{12}C, ^{8}Be\rightarrow 2\alpha)^{16}O$ reaction.

The Makrofol detector of the ^{11}B-target bombardment was very clean, with practically no tracks in the ^{8}Be-group range. This fact excludes the contribution not only from the ^{11}B contaminant but also from anything originating outside the target, such as the contribution from the reactions in the absorber before the Makrofol detector.

The Makrofol detector of the ^{9}Be-target bombardment had a large, but countable, number of tracks. The large yield arose from the $^{12}C+^{9}Be\rightarrow ^{13}C(3.09\ MeV)+(^{8}Be\rightarrow 2\alpha)$ neutron transfer reaction, which occurs[17] with large cross sections at low energies due to the favorable Q value. From the observed track density, the ^{13}C 3.09-MeV γ-ray yield in the $^{12}C+^{9}Be$ bombardment, and the fact that the ^{13}C 3.09-MeV γ ray was not seen in the $^{12}C+^{12}C$ bombardment, the possible contribution to the $^{8}Be\rightarrow 2\alpha$ yield from the ^{9}Be contaminant in the ^{12}C target was estimated to be less that 2% of the actual counts.

The Makrofol detector of the Li-target bombardment had a huge, uncountable number of tracks, due to the scattered Li nuclei, which were not completely stopped in the absorbers. As we have no reason to believe that our carbon targets would contain more Li than Be contaminant, and as the HPG spectra of $^{12}C+^{12}C$ bombardment show no characteristic γ rays of the $^{7}Li+^{12}C\rightarrow\alpha+^{15}N$ reaction, we are inclined to exclude the importance of the Li contaminant as well.

The hydrogen contaminant is unimportant since the $p+^{12}C$ reaction does not result in α particles. The ^{4}He in the target would, by elastic scattering of the ^{12}C beam particles, result in an angular distribution peaked at backward angles, which is in contradiction with the observed angular distribution which is sharply peaked forward. We therefore conclude that the relative increase in the $^{12}C(^{12}C,^{8}Be)^{16}O$ cross section at the energies $E_{c.m.}\leq 3.13$ MeV cannot be attributed to a target contaminant. Morever, the fact that the ^{8}Be angular distributions measured at $E_{c.m.}=3.13$ MeV and $E_{c.m.}=3.91$ MeV are very similar (Figs. 8 and 9) also indicates that the $^{8}Be\rightarrow 2\alpha$ group at $E_{c.m.}=3.13$ MeV does not contain spurious counts. Thus we conclude that our $^{12}C(^{12}C,^{8}Be)^{16}O$ cross-section measurements are correct within the errors given by the dispersion of results, obtained by the two types of analysis and the two different normalizations (Fig. 11).

Comparing the ratio of the measured ^{8}Be and α_0 yields with the compound-nucleus statistical-evaporation estimate, we note that it exceeds the statistical estimate by a factor of 15 to 50 at $5.24\geq E_{c.m.}\geq 3.91$ MeV and a factor of $\sim 10^{5}$ to 10^{8} at $3.13\geq E_{c.m.}\geq 2.43$ MeV. Considering $^{12}C(^{12}C,^{8}Be)^{16}O$ a direct α-transfer reaction, the cross section $\sigma(E)$ has been evaluated for the $l=0$ transfer in the distorted-wave Born approximation (DWBA) with the LOLA program, using the "standard" optical-model potential ($V_0=-50$ MeV, $W=-10$ MeV, $R=1.26(A_1^{1/3}+A_2^{1/3})$ fm, and $a=0.4$ fm) in the ingoing and outgoing channels. The evaluated $\sigma(E)=S_1S_2\sigma_{LOLA}(E)$ is shown in Fig. 11, with the theoretical spectroscopic factors, $S_1(^{12}C\rightarrow ^{8}Be+\alpha)=0.285$ and $S_2(^{16}O\rightarrow ^{12}C+\alpha)=0.104$ of Ichimura *et al.*[18] As seen in Fig. 11, the DWBA α-transfer prediction reproduces the experimental cross sections quite well down to incident energy $E_{c.m.}=3.91$ MeV, but underpredicts them by one to three orders of magnitude at $3.13\geq E_{c.m.}\geq 2.43$ MeV. A similar effect occurs in the $^{11}B(^{9}Be,^{8}Be)^{15}N$ transfer reaction, where an enhancement is observed[11] relative to the DWBA prediction at incident energies $2.0\geq E_{c.m.}\geq 1.4$ MeV. The present measurements of the $^{12}C(^{12}C,^{8}Be)^{16}O$ cross section thus clearly indicate, with the observed change in slope at $E_{c.m.}\approx 3.5$ MeV and the large enhancement at lower energies, that another mechanism, most plausibly that of the formation of ^{12}C-^{12}C dinuclear states, favoring an α transfer, becomes predominant at energies $E_{c.m.}\leq 3.13$ MeV.

IV. CONCLUSIONS

In the present work we measured the differential cross sections for the $^{12}C(^{12}C,^{8}Be)^{16}O$ reaction at eight incident energies in the range $2.43\leq E_{c.m.}\leq 5.24$ MeV.

All measured angular distributions are characterized by contributions of $l=0$ and $l=2$ partial waves. The integrated cross sections extend to over 6 orders of magnitude, from 4×10^{-4} μb to 280 μb.

Down to $E_{c.m.}\approx 4$ MeV, the $^{12}C(^{12}C,^{8}Be)^{16}O$ cross section is smaller and decreases with decreasing incident energy more rapidly than the $^{12}C(^{12}C,\alpha_0)^{20}Ne$ cross section. At $E_{c.m.}\leq 3.13$ MeV, however, it becomes larger than the $^{12}C(^{12}C,\alpha_0)^{20}Ne$ cross section, though it does not exceed the "total reaction" cross section, including all α and proton channels.

The observed change in the slope at $E_{c.m.}\approx 3.5$ MeV and the large enhancement at lower energies over both the statistical and the direct α-transfer prediction clearly indicate that another mechanism, most plausibly that of the formation of ^{12}C-^{12}C dinuclear states favoring an α transfer, becomes predominant at energies $E_{c.m.}\leq 3.13$ MeV.

ACKNOWLEDGMENTS

Our thanks are due to Professor J. A. Cameron and Dr. B. Dasmahapatra for their help in performing some measurements with the Fowler-Nordheim (FN) tandem accelerator of McMaster University and to Dr. Q. Haider for performing the distorted wave Born approximation (DWBA) calculations. This work was supported in part by the Natural Sciences and Engineering Research Council of Canada.

*Permanent address: Institute of Nuclear Research of the Hungarian Academy of Sciences, H-4001 Debrecen, Hungary.

[1]E. Almqvist, D. A. Bromley, and J. A. Kuehner, Phys. Rev. Lett. **4**, 515 (1960); D. A. Bromley, J. A. Kuehner, and E. Almqvist, Phys. Rev. Lett. **4**, 365 (1960); Phys. Rev. **123**, 878 (1961).

[2]J. R Patterson, H. Winkler, and C. S. Zaidins, Astrophys. J. **157**, 367 (1968); M. G. Mazarakis and W. E. Stephens, Phys. Rev. **7**, 1280 (1973).

[3]H. W. Becker, K. U. Kettner, C. Rolfs, and H. P. Trautvetter, Z. Phys. A **303**, 305 (1981).

[4]M. D. High and B. Čujec, Nucl. Phys. **282**, 181 (1977).

[5]K. U. Kettner, H. Lorentz-Wirzba, and C. Rolfs, Z. Phys. A **298**, 65 (1980).

[6]N. R. Fletcher, J. D. Fox, G. J. Kekelis, G. R. Morgan, and G. A. Norton, Phys. Rev. C **13**, 1173 (1976).

[7]R. Wada, T. Murakami, E. Takada, M. Fukada, and K. Takimoto, Phys. Rev. C **22**, 557 (1980).

[8]D. Sprengel, H. V. Buttlar, J. Dreverman, W. Hoppe, R. Esenbügel, E. U. Klauss, and N. Markardt, Adriatic International Conference on Nuclear Physics, Hvar, 1984 [Fiz. (Zagreb) Suppl. 1, **16**, 25 (1984)].

[9]Ben-Zion Kozlovski, Astrophys. Space Sci. **8**, 114 (1970).

[10]A. Gobbi and D. A. Bromley, in *Heavy Ion Collisions*, edited by R. Bock (North-Holland, Amsterdam, 1979), Vol. 1.

[11]B. Čujec, B. Dasmahapatra, Q. Haider, F. Lahlou, and R. Dayras, Nucl. Phys. **453**, 505 (1986).

[12]I. Hunyadi, I. M. Szöghy, and B. Čujec, Proceedings of the 12th International Conference on Solid State Nuclear Track Detectors, Acapulco, 1983 [Nucl. Tracks Rad. Meas. **8**, 525 (1984)].

[13]G. Somogyi, I. Hunyadi, E. Koltay, and L. Zolnai, Nucl. Instrum. Methods **147**, 287 (1977).

[14]I. M. Szöghy, Q. Haider, and R. Ouellet, Nucl. Instrum. Methods **A242**, 277 (1986).

[15]B. K. Dasmahapatra, B Čujec, and F. Lahlou, Lett. Nuovo Cimento **35**, 345 (1982).

[16]R. K. Hobbie and F. F. Forbes, Phys. Rev. **126**, 2137 (1962).

[17]H. Cheung, M. D. High, and B. Čujec, Nucl. Phys. **A296**, 333 (1978).

[18]M. Ichimura, A. Arima, E. C. Halbert, and T. Terasawa, Nucl. Phys. **A204**, 225 (1973).